COORDINATE PERTURBATION METHOD FOR UPPER BOUND LIMIT ANALYSIS

J.P. Hambleton & S.W. Sloan
Centre for Geotechnical and Materials Modelling, University of Newcastle, Newcastle, NSW, Australia

ABSTRACT: *Conventional methods for numerical upper bound limit analysis utilize a predefined mesh of elements with nodes at fixed coordinates, and there the objective is to find the kinematically admissible velocity field associated with the mesh that minimizes the limit load. In this paper, a numerical method for optimizing the applied load with respect to both the velocity field and nodal coordinates is presented. The formulation is for the classical case of rigid elements (blocks) separated by velocity discontinuities, considering plane strain and weightless material obeying the Mohr-Coulomb yield condition. The central idea of the approach is to successively perturb velocities and nodal coordinates starting from an initial solution corresponding to a predefined mesh, where the equations governing the perturbed velocities and nodal coordinates are derived through linearization of exact expressions of the limit load and the conditions imposed on velocity jumps by the flow rule. Despite approximations made in perturbation steps, the method furnishes a final solution which satisfies the flow rule and energy balance exactly (within numerical tolerances) and therefore provides a rigorous upper bound on the true collapse load. The effectiveness of the method is demonstrated by comparing numerical results with the analytical solution for a benchmark problem in soil mechanics.*

1 INTRODUCTION

Upper bound limit analysis, otherwise known as the kinematic method of limit analysis, is a rigorous and effective means of evaluating collapse loads of structures and the soils/rocks on which they rest. As discussed in depth by Chen (1975), the technique applies to perfectly plastic materials whose flow rule obeys normality (associativity), and it hinges on constructing a kinematically admissible velocity field (collapse mechanism) for a given problem, where kinematic admissibility implies that the plastic flow rule and boundary conditions are satisfied. By balancing the rate of work dissipated within the material to the rate of work done by external forces, one may evaluate a load which is a rigorous bound on the true collapse load. This bound is an upper bound for loads inducing collapse (the case usually considered in the literature) and a lower bound for loads resisting collapse.

Limit analysis has origins as an elegant analytical or semi-analytical technique, and it continues to be used in this context to this day (e.g., Michalowski, 1997, 2004, 2007; Soubra, 1999, Maciejewski & Jarzębowski, 2004; Soon & Drescher, 2007; Hambleton & Drescher, 2011). Analytical works often employ a collapse mechanism consisting of rigid blocks separated by velocity discontinuities, where a velocity discontinuity is regarded as a material layer of vanishing thickness across which a jump in velocity occurs (Chen 1975). In this

approach, kinematic admissibility is ensured from the outset by composing a hodograph, or velocity diagram, in which velocity jumps between rigid blocks satisfy the condition imposed by the flow rule. The mechanism usually consists of free variables that can assume any value within a certain range (e.g., interior angles of the blocks), and thus an optimization procedure is employed to find values of these free variables that minimize the collapse load. For very simple mechanisms the minimum can be found analytically, but in general it is necessary to employ a numerical optimization scheme that is suitable for a general nonlinear objective function (e.g., Levenberg–Marquardt algorithm).

The concepts of limit analysis also have been utilized as the basis for efficient numerical methods (e.g., Anderheggen & Knöpfel, 1972; Bottero et al., 1980; Sloan & Kleeman 1995; Lyamin & Sloan, 2002; Chen et al. 2003; Krabbenhøft et al., 2005; Makrodimopoulos & Martin, 2007, 2008; Smith & Gilbert, 2007). With the exception of the work by Smith & Gilbert (2007), these numerical approaches rest on discretizing the problem domain using finite elements and then minimizing the load (again evaluated via energy balance) subject to constraints on the interpolated velocity field imposed by the flow rule and boundary conditions. The velocity field typically varies continuously within each element using linear or quadratic interpolation of nodal velocities, and element edges correspond to velocity discontinuities. In contrast to semi-analytical limit analysis, in which the number of free variables is quite limited, procedures for numerical limit analysis are able to take advantage of large-scale optimization schemes such as conic programming, which can efficiently operate with thousands or hundreds of thousands of free variables.

A central difference between the analytical and numerical forms of limit analysis is that the optimal location of discontinuities is usually determined as part of the solution procedure in the analytical method, whereas any discontinuities present in numerical methods have a fixed position as a consequence the mesh being predefined. Indeed, numerical methods usually allow for arbitrarily complex zones of continuous deformation but are incapable of reproducing global velocity discontinuities present in a collapse mechanism unless the location of the discontinuity is known a priori, in which case element edges can be aligned with the known discontinuity as part of the procedure for mesh generation. The formulation proposed by Smith & Gilbert (2007), which is not a finite element method, revolves around finding the optimal location of discontinuities by searching over a large set of potential locations obtained from connecting nodes of a grid laid out over the problem domain.

In this paper, a method for finding the optimal location of discontinuities using finite elements is introduced. The formulation is based on successively perturbing velocities and nodal coordinates beginning from an initial solution, where the initial solution is obtained from a predefined mesh of finite elements using well-established procedures for numerical limit analysis. The formulation presented is for triangular rigid elements (plane strain) separated by velocity discontinuities, and it is therefore identical to the classical limit analysis method employing sliding rigid blocks (cf. Chen 1975). Indeed, the terms “element” and “block” are viewed as being interchangeable, and “nodes” of the finite element mesh are none other than the vertices of the triangular blocks. It is assumed in this paper that the material is homogenous and characterized by the Mohr-Coulomb yield condition, with friction angle and cohesion denoted ϕ and c, respectively. Furthermore, the material is considered to be weightless, although it is possible to include body forces in the formulation (Hambleton & Sloan, 2011).

In Section 2, exact expressions of the conditions on velocity jumps between elements, as well are the limit load, are derived. The proposed numerical formulation based on the perturbation method is presented in Section 3, and its application to the benchmark problem of passive earth pressure behind a smooth retaining wall is considered in the penultimate

section. Detailed analysis of the proposed numerical method, as well as additional examples and verifications, will be provided in a forthcoming paper (Hambleton & Sloan, 2011).

2 GENERAL EQUATIONS FOR SLIDING RIGID ELEMENTS

As in analytical methods for limit analysis (cf. Chen 1975), the proposed formulation is based on splitting the problem domain into a number of rigid triangular elements whose edges correspond to velocity discontinuities. The initial finite element mesh is chosen somewhat arbitrarily, although it should be emphasized that it is possible to select an initial mesh for which no kinematically admissible velocity field exists. Here it is assumed that an admissible velocity field exists for the initial mesh.

Fig. 1 shows the line segment corresponding to a velocity discontinuity at the edge shared by two adjacent elements in a finite element mesh. Each discontinuity, or edge, is assigned a global number that is designated by the index k (k = 1,2,…,N_{edges}, where N_{edges} is the total number of edges). Using the convention shown in Fig. 1, the subscripts i and j denote quantities in the elements adjacent to edge k, as well as the nodes corresponding to the endpoints of the edge. Velocity vectors in the elements associated with discontinuity k are denoted as

$$\mathbf{v}_i = \begin{bmatrix} v_{x,i} & v_{y,i} \end{bmatrix}^T, \qquad \mathbf{v}_j = \begin{bmatrix} v_{x,j} & v_{y,j} \end{bmatrix}^T \tag{1}$$

In Eq. (1), $v_{x,i}$ and $v_{y,i}$ are components of velocity in the x-direction and y-direction (Fig. 1), respectively, for element i, and $v_{x,j}$ and $v_{y,j}$ are components of velocity for element j. Node i is located at coordinates (x_i,y_i), and coordinates of node j are (x_j,y_j).

In the sections that follow the condition imposed by the flow rule on velocity jumps between elements is derived, as well as an expression of the limit load based on balancing the total rate of work done by external forces with the total rate of dissipation within the material.

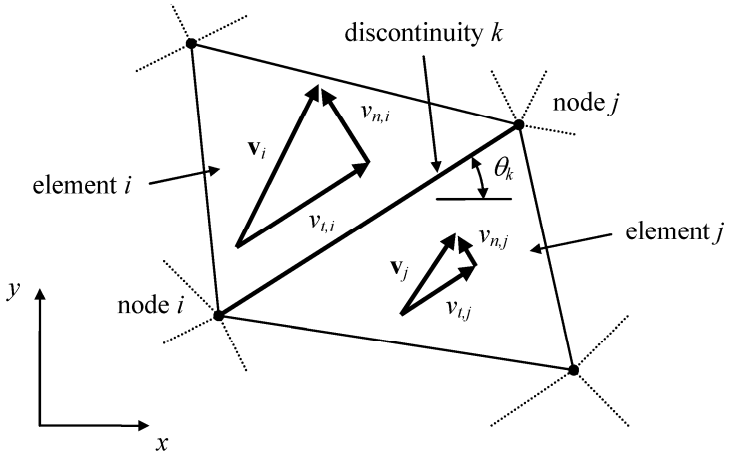

Fig. 1. Notation for a discontinuity (element edge) and velocities in adjacent elements (all quantities positive as drawn)

2.1 Jump condition

The associated flow rule for the Mohr-Coulomb yield condition requires that the jump in velocity between elements satisfies the following condition (Chen 1975)

$$\Delta v_{n,k} = \left|\Delta v_{t,k}\right| \tan\phi \tag{2}$$

where $\Delta v_{n,k}$ and $\Delta v_{t,k}$ are, respectively, jumps in the components of velocity normal and tangential to discontinuity k. The jumps are calculated as

$$\Delta v_{n,k} = v_{n,i} - v_{n,j}, \qquad \Delta v_{t,k} = v_{t,i} - v_{t,j} \tag{3}$$

where v_n and v_t denote components of velocity in directions normal and tangential to the discontinuity, with subscript i or j indicating the element (see Fig. 1). These components are related to components in the x-y system through

$$v_{n,i} = -v_{x,i}\sin\theta_k + v_{y,i}\cos\theta_k, \qquad v_{t,i} = v_{x,i}\cos\theta_k + v_{y,i}\sin\theta_k \tag{4}$$

$$v_{n,j} = -v_{x,j}\sin\theta_k + v_{y,j}\cos\theta_k, \qquad v_{t,j} = v_{x,j}\cos\theta_k + v_{y,j}\sin\theta_k \tag{5}$$

In Eqs. (4) and (5), θ_k is the angle at which the edge is inclined from the horizontal, considering the endpoint specified by subscript i as the origin (Fig. 1). The trigonometric functions in (4) and (5) are given by

$$\cos\theta_k = \frac{x_j - x_i}{l_k}, \qquad \sin\theta_k = \frac{y_j - y_i}{l_k} \tag{6}$$

where l_k is the length of the discontinuity evaluated as

$$l_k = \sqrt{\left(x_j - x_i\right)^2 + \left(y_j - y_i\right)^2} \tag{7}$$

Upon substitution of the expressions from Eqs. (3)-(6), the jump condition of Eq. (2) can be written as

$$-v_{x,i}\left(y_j - y_i\right) + v_{y,i}\left(x_j - x_i\right) + v_{x,j}\left(y_j - y_i\right) - v_{y,j}\left(x_j - x_i\right) = \alpha_k \tan\phi \tag{8}$$

where

$$\alpha_k = l_k\left|\Delta v_{t,k}\right| = \left|v_{x,i}\left(x_j - x_i\right) + v_{y,i}\left(y_j - y_i\right) - v_{x,j}\left(x_j - x_i\right) - v_{y,j}\left(y_j - y_i\right)\right| \tag{9}$$

It may be noted that the length l_k cancels in the final expressions of the jump condition given by Eqs. (8) and (9), which later on simplifies the process of linearization significantly.

2.2 Energy balance

Dissipation for the mechanism involving rigid blocks comes exclusively from velocity discontinuities, where dissipation for a single discontinuity is calculated as (Chen 1975)

$$d_k = c l_k\left|\Delta v_{t,k}\right| = c\alpha_k \tag{10}$$

In this paper, body forces are neglected, and the rate of work done by external forces involves only surface tractions. For simplicity, it is now further assumed that the rate of work done by

surface tractions comes only from the (unknown) limit load. That is, fixed tractions outside the region where the limit load is applied (i.e., surcharges) are zero. With this the total balance of energy requires simply

$$c\sum_{k=1}^{N_{edges}}\alpha_k = \int_S \left(t_x v_x + t_y v_y\right) ds \tag{11}$$

where t_x and t_y are, respectively, tractions in the x-direction and y-direction corresponding to the limit load and S is the part of the surface over which these tractions are applied.

Eq. (11) is generally applicable to a problem with no body forces or surcharge, although further information must be given in order to define the limit load explicitly. In the example considered later in Section 4, it is assumed that $v_y = 0$ and $v_x = v_0$, where v_0 is an arbitrary constant (usually taken as unity for convenience). These assumptions correspond simple translation in the x-direction, and for this case total force in the x-direction, denoted P, represents the limit load. Upon manipulating Eq. (11), the expression for P is

$$P = \int_S t_y ds = \frac{c}{v_0}\sum_{k=1}^{N_{edges}}\alpha_k \tag{12}$$

Thus, the quantity on the right-hand side of Eq. (12) is identically equal to the limit load that one wishes to minimize. Alternatives to Eq. (12) for other loading scenarios can be readily derived.

3 PERTURBATION METHOD

To determine the optimal location of velocity discontinuities, nodal coordinates defining the positions of the discontinuities must be included with the velocities as free variables (unknowns). For a single discontinuity the free variables can be combined in a single vector, $\mathbf{x}_k$, defined as

$$\mathbf{x}_k = \begin{bmatrix} x_i & y_i & x_j & y_j & v_{x,i} & v_{y,i} & v_{x,j} & v_{y,j} \end{bmatrix}^T \tag{13}$$

With a view towards implementing a standard large-scale optimization scheme (e.g., conic programming), equality constraints and an objective function that are linear with respect to the free variables are required. Since the jump condition and expression of the limit load (Eqs. (8) and (12)) are nonlinear with respect to the free variables, it is necessary to work with linear approximations rather than the exact expressions. A tacit assumption is that there is a known point $\mathbf{x}_k^0$ about which the equations can be linearized. Initially, the point $\mathbf{x}_k^0$ corresponds to the solution found using fixed coordinates, i.e., one obtained using well-established methods for numerical limit analysis (e.g., Krabbenhøft et al., 2005; Makrodimopoulos & Martin, 2008), and the concept of the proposed numerical method is to "perturb" both velocities and nodal coordinates from this initial solution using linear approximations of Eqs. (8) and (12). Upon finding a new solution with updated nodal coordinates, the velocities and nodal coordinates may again be perturbed by a small amount, and in this way the proposed scheme is incremental.

3.1 Linear approximations

In order to linearize the jump condition of Eq. (8), the equality is first written in the form $F(\mathbf{x}_k) = 0$, where the function $F(\mathbf{x}_k)$ is defined as

$$F(\mathbf{x}_k) = -v_{x,i}(y_j - y_i) + v_{y,i}(x_j - x_i) + v_{x,j}(y_j - y_i) - v_{y,j}(x_j - x_i) - \alpha_k \tan\phi \tag{14}$$

The linear approximation of the jump condition is then obtained by a first-order Taylor series expansion of $F(\mathbf{x}_k)$ about the point $\mathbf{x}_k^0$, viz.

$$F(\mathbf{x}_k) \approx F(\mathbf{x}_k^0) + (\mathbf{x}_k - \mathbf{x}_k^0)^T \left.\frac{\partial F}{\partial \mathbf{x}_k}\right|_{\mathbf{x}_k = \mathbf{x}_k^0} \tag{15}$$

Upon evaluating the derivative and performing some manipulation, Eq. (15) can be expressed as

$$\begin{aligned} F(\mathbf{x}_k) \approx\ & -v_{x,i}^0 \Delta y + v_{y,i}^0 \Delta x + v_{x,j}^0 \Delta y - v_{y,j}^0 \Delta x - v_{x,i} \Delta y^0 + v_{y,i} \Delta x^0 + v_{x,j} \Delta y^0 - v_{y,j} \Delta x^0 \\ & + v_{x,i}^0 \Delta y^0 - v_{y,i}^0 \Delta x^0 - v_{x,j}^0 \Delta y^0 + v_{y,j}^0 \Delta x^0 - D(\mathbf{x}_k) \tan\phi \end{aligned} \tag{16}$$

where

$$\Delta x = x_j - x_i, \quad \Delta y = y_j - y_i, \quad \Delta x^0 = x_j^0 - x_i^0, \quad \Delta y^0 = y_j^0 - y_i^0 \tag{17}$$

In Eqs. (16) and (17), the superscript "0" is used to indicate quantities corresponding the point $\mathbf{x}_k^0$ about which linearization is performed, and the function $D(\mathbf{x}_k)$ is the linear approximation of α_k defined as

$$\alpha_k(\mathbf{x}_k) \approx D(\mathbf{x}_k) = \alpha_k(\mathbf{x}_k^0) + (\mathbf{x}_k - \mathbf{x}_k^0)^T \left.\frac{\partial \alpha_k}{\partial \mathbf{x}_k}\right|_{\mathbf{x}_k = \mathbf{x}_k^0} \tag{18}$$

Upon manipulation, the function $D(\mathbf{x}_k)$ can be reduced to the following

$$\begin{aligned} D(\mathbf{x}_k) = \langle & v_{x,i}^0 \Delta x^0 + v_{y,i}^0 \Delta y^0 - v_{x,j}^0 \Delta x^0 - v_{y,j}^0 \Delta y^0 \rangle \big[v_{x,i}^0 \Delta x + v_{y,i}^0 \Delta y - v_{x,j}^0 \Delta x - v_{y,j}^0 \Delta y \\ & + v_{x,i} \Delta x^0 + v_{y,i} \Delta y^0 - v_{x,j} \Delta x^0 - v_{y,j} \Delta y^0 - v_{x,i}^0 \Delta x^0 - v_{y,i}^0 \Delta y^0 + v_{x,j}^0 \Delta x^0 + v_{y,j}^0 \Delta y^0 \big] \end{aligned} \tag{19}$$

where $\langle \bullet \rangle$ is the sign function defined as

$$\langle \xi \rangle = \begin{cases} 1 & \text{for } \xi > 0 \\ -1 & \text{for } \xi < 0 \\ \text{undefined} & \text{for } \xi = 0 \end{cases} \tag{20}$$

The expression for the limit load, Eq. (12), is a linear combination of α_k (k = 1,2,…,N_{edges}) and is also therefore linearized by replacing α_k with $D(\mathbf{x}_k)$.

An attempt to use Eq. (19) directly will in general lead to difficulties in the numerical scheme. The equation is undefined, for example, in the case when velocities are zero in both elements adjacent to a discontinuity. Furthermore, it is a basic requisite that dissipation is positive. Rather than use the expression for $D(\mathbf{x}_k)$ from Eq. (19), the following definition is therefore adopted

$$D(\mathbf{x}_k) = \left| v^0_{x,i}\Delta x + v^0_{y,i}\Delta y - v^0_{x,j}\Delta x - v^0_{y,j}\Delta y + v_{x,i}\Delta x^0 + v_{y,i}\Delta y^0 - v_{x,j}\Delta x^0 - v_{y,j}\Delta y^0 \right.$$
$$\left. - v^0_{x,i}\Delta x^0 - v^0_{y,i}\Delta y^0 + v^0_{x,j}\Delta x^0 + v^0_{y,j}\Delta y^0 \right| \tag{21}$$

Unlike the linear approximation, Eq. (21) leads to a robust numerical formulation even when the jump in the tangential component of velocity, $\Delta v_{t,k}$, becomes zero or changes sign. It may be noted that Eq. (21) is identical to the linear approximation of α_k provided $\Delta v_{t,k}$ does not change sign during a perturbation step.

3.2 Optimization and solution stepping

As indicated in the introduction to Section 3, the concept of the numerical formulation is to perform a number of steps in which the nodal coordinates and velocities are perturbed by a small amount, starting from an initial solution corresponding to a predefined mesh. Each perturbation step corresponds to a constrained optimization problem where the goal is to minimize the limit load (Eq. (12) with α_k replaced by $D(\mathbf{x}_k)$) subject to the equality constraints corresponding to jump conditions ($F(\mathbf{x}_k) = 0$, where $F(\mathbf{x}_k)$ is given by Eq. (16)).

The motivation for using a relatively large number of small perturbations, as opposed to a small number of large perturbations, is twofold. First, the linear approximations from Section 3.1 are valid only for small variations in the free variables. Second, the connectivity of the element mesh must remain unchanged as the nodal coordinates are adjusted, and allowing nodal coordinates to change substantially will invariably lead to mesh degeneration (e.g., elements with negative volume). By arriving at a final solution through a number of small steps, mesh degeneration is not necessarily prevented, but the method will at least furnish the best possible solution prior to the mesh becoming invalid. To ensure that the adjustment to the solution is small in each step, the following radial constraint on the nodal coordinates is introduced

$$\rho_{\max,m} \geq \sqrt{\left(x_m - x^0_m\right)^2 + \left(y_m - y^0_m\right)^2} \tag{22}$$

where m indicates the global node number ($m = 1,2,\ldots,N_{nodes}$, where N_{nodes} is the total number of nodes) and $\rho_{\max,m}$ is a specified maximum radius. The parameter $\rho_{\max,m}$ should be taken as a small fraction of the element length and may in general be different for each node.

In this paper optimization was performed using the Matlab toolbox SeDuMi. Among other functions, this software package efficiently solves large-scale constrained optimization problems using second-order cone programming (Sturm 1999), which accommodates so-called "quadratic, second-order cone constraints" of the type given in Eq. (22). As discussed by Lyamin et al. (2004), such constraints also can be introduced to handle the absolute value appearing in the equations for the jump condition and dissipation. This is accomplished by everywhere replacing $D(\mathbf{x}_k)$ with the variable μ_k ($k = 1,2,\ldots,N_{edges}$), which is constrained as follows

$$\mu_k \geq \sqrt{\lambda_k^2} \tag{23}$$

where

$$\lambda_k = v^0_{x,i}\Delta x + v^0_{y,i}\Delta y - v^0_{x,j}\Delta x - v^0_{y,j}\Delta y + v_{x,i}\Delta x^0 + v_{y,i}\Delta y^0 - v_{x,j}\Delta x^0 - v_{y,j}\Delta y^0$$
$$- v^0_{x,i}\Delta x^0 - v^0_{y,i}\Delta y^0 + v^0_{x,j}\Delta x^0 + v^0_{y,j}\Delta y^0 \tag{24}$$

The variable λ_k is simply the expression appearing in the absolute value in Eq. (21), such that $D(\mathbf{x}_k) = |\lambda_k|$. In order to force the algorithm to find a solution with $\mu_k = D(\mathbf{x}_k)$, the expression for the limit load (Eq. (12)) is replaced by

$$P = \frac{c}{v_0} \sum_{k=1}^{N_{edges}} \mu_k \tag{25}$$

By using Eq. (25) as the objective function, the global minimum for the problem corresponds to $\mu_k = D(\mathbf{x}_k)$ by construction.

To write the optimization problem for a perturbation step in the canonical form used by SeDuMi and other solvers, the following global vector of unknowns is defined

$$\mathbf{x} = \begin{bmatrix} \mathbf{x}_{crd}^T & \mathbf{x}_{vel}^T & \mathbf{x}_{\alpha\beta}^T & \mathbf{x}_{\rho}^T \end{bmatrix}^T \tag{26}$$

where

$$\mathbf{x}_{crd} = \begin{bmatrix} x_1 & y_1 & x_2 & y_2 & \dots & x_{N_{nodes}} & y_{N_{nodes}} \end{bmatrix}^T \tag{27}$$

$$\mathbf{x}_{vel} = \begin{bmatrix} v_{x,1} & v_{y,1} & v_{x,2} & v_{y,2} & \dots & v_{x,N_{elems}} & v_{y,N_{elems}} \end{bmatrix}^T \tag{28}$$

$$\mathbf{x}_{\mu\lambda} = \begin{bmatrix} \mu_1 & \lambda_1 & \mu_2 & \lambda_2 & \dots & \mu_{N_{edges}} & \lambda_{N_{edges}} \end{bmatrix}^T \tag{29}$$

$$\mathbf{x}_{\rho} = \begin{bmatrix} \rho_{\max,1} & \rho_{x,1} & \rho_{y,1} & \rho_{\max,2} & \rho_{x,2} & \rho_{y,2} & \cdots & \rho_{\max,N_{nodes}} & \rho_{y,N_{nodes}} & \rho_{y,N_{nodes}} \end{bmatrix}^T \tag{30}$$

In Eq. (28), N_{elems} is the total number of elements, and in Eq. (30) the variables $\rho_{x,m}$ and $\rho_{y,m}$ ($m = 1,2,\dots,N_{nodes}$) are defined as

$$\rho_{x,m} = x_m - x_m^0 \tag{31}$$

$$\rho_{y,m} = y_m - y_m^0 \tag{32}$$

The canonical form of the optimization problem is then

$$\begin{aligned} &\text{minimize} && \mathbf{c}^T\mathbf{x} \\ &\text{such that} && \mathbf{A}\mathbf{x} = \mathbf{b} \\ & && \mu_k \geq \sqrt{\lambda_k^2} \quad \text{for } k = 1,2,\dots,N_{edges} \\ & && \rho_{\max,m} \geq \sqrt{\rho_{x,m}^2 + \rho_{y,m}^2} \quad \text{for } m = 1,2,\dots,N_{nodes} \end{aligned} \tag{33}$$

Referring to the objective function of Eq. (25), the vector of constants $\mathbf{c}$ is given by

$$\mathbf{c} = \frac{c}{v_0}[\underbrace{0 \quad 0 \quad \dots \quad 0}_{1\times(2N_{nodes}+2N_{elems})} \quad \underbrace{1 \quad 0 \quad 1 \quad 0 \quad \dots \quad 1 \quad 0}_{1\times 2N_{edges}} \quad \underbrace{0 \quad 0 \quad \dots \quad 0}_{1\times 3N_{nodes}}]^T \tag{34}$$

The matrix of constants $\mathbf{A}$ and vector of constants $\mathbf{b}$ are determined by assembling (1) jump conditions for all discontinuities, (2) definitions of auxiliary variables, and (3) constraints required to fix nodal coordinates and velocities for a particular problem. The jump conditions are simply $F(\mathbf{x}_k) = 0$ ($k = 1,2,\dots,N_{nodes}$), where $F(\mathbf{x}_k)$ is given by Eq. (16) with $D(\mathbf{x}_k)$ replaced by μ_k. The auxiliary variables are λ_k, $\rho_{x,m}$, and $\rho_{y,m}$, and they are defined by Eqs. (24), (31), and (32), respectively.

An arbitrary number of perturbation steps can be performed in the analysis of a problem. In each step, the variables with a superscript "0" are regarded as known quantities from the previous step, and the solution of (33) yields the values of unknowns at the end of the step. A natural stopping criterion in this stepping procedure is for the variation of the limit load within an increment to be below some tolerance, although other criteria can be implemented.

Finally, it is noted that by fixing all nodal coordinates as the values at the beginning of a perturbation step ($x_i = x_i^0$, $y_i = y_i^0$, etc.), exact expressions of the jump condition and energy balance (Eqs. (8) and (12)) are recovered from the linear approximations, and in this case, the only unknowns are the velocities. Fixing the nodal coordinates thus provides a means for obtaining a solution for the initial mesh, and it can also be used to obtain an exact solution (within numerical tolerances) for the limit load at any solution step.

4 EXAMPLE

In this section the proposed numerical formulation is applied to a classical problem in soil mechanics: passive earth pressure behind a smooth retaining wall. The wall has height H and translates into weightless material with friction angle $\phi = 10^\circ$. For simplicity, the maximum variation in nodal coordinates the same for all nodes and fixed at $H/100$ (i.e, $\rho_{\max,m} = H/100$ for $m = 1,2,\ldots,N_{nodes}$).

The initial finite element mesh for the problem is shown in Fig. 2 (indicated by "step number = 0"). Superimposed on the mesh are the element velocities obtained by fixing nodal coordinates at their initial values in the numerical formulation. The collapse mechanism for the initial mesh is considerably different than the one predicted analytically in the Coulomb theory of lateral earth pressure, which corresponds to the single discontinuity indicated by a dashed line in Fig. 2.

Fig. 2 also shows the finite element mesh and velocities after 20, 40, and 60 perturbation steps. The collapse mechanism becomes progressively closer to the Coulomb solution with the number of perturbation steps, and when the step number is 60, it is virtually indistinguishable from the analytical result.

Fig. 3 compares the limit load evaluated numerically with the analytical solution of $P/cH \approx 2.3835$. The limit load evaluated for the initial mesh is $P/cH \approx 13.0965$, over 5 times larger than the analytical prediction, but it rapidly approaches the analytical result as the stepping procedure proceeds. At step number 55, the numerical and analytical predictions are in agreement to all four decimal places given.

5 CONCLUDING REMARKS

The paper presents a numerical method for upper bound limit analysis in which both velocities and the location of velocity discontinuities are optimized simultaneously. The method is based on successively perturbing the velocities and nodal coordinates, starting from solution that can be obtained by conventional techniques for numerical limit analysis. The formulation presented is for collapse mechanisms consisting of sliding rigid elements (blocks) separated by velocity discontinuities, although it is expected that the approach can be generalized to finite element formulations involving continuous deformation within elements. Simulation of a benchmark problem in soil mechanics indicates that the method is robust and capable of recovering the exact (analytical) solution even when the collapse mechanism for the initial finite element mesh is significantly different from the optimal one. Additional verifications and analysis of the numerical formulation will be given in an upcoming journal paper (Hambleton & Sloan, 2011).

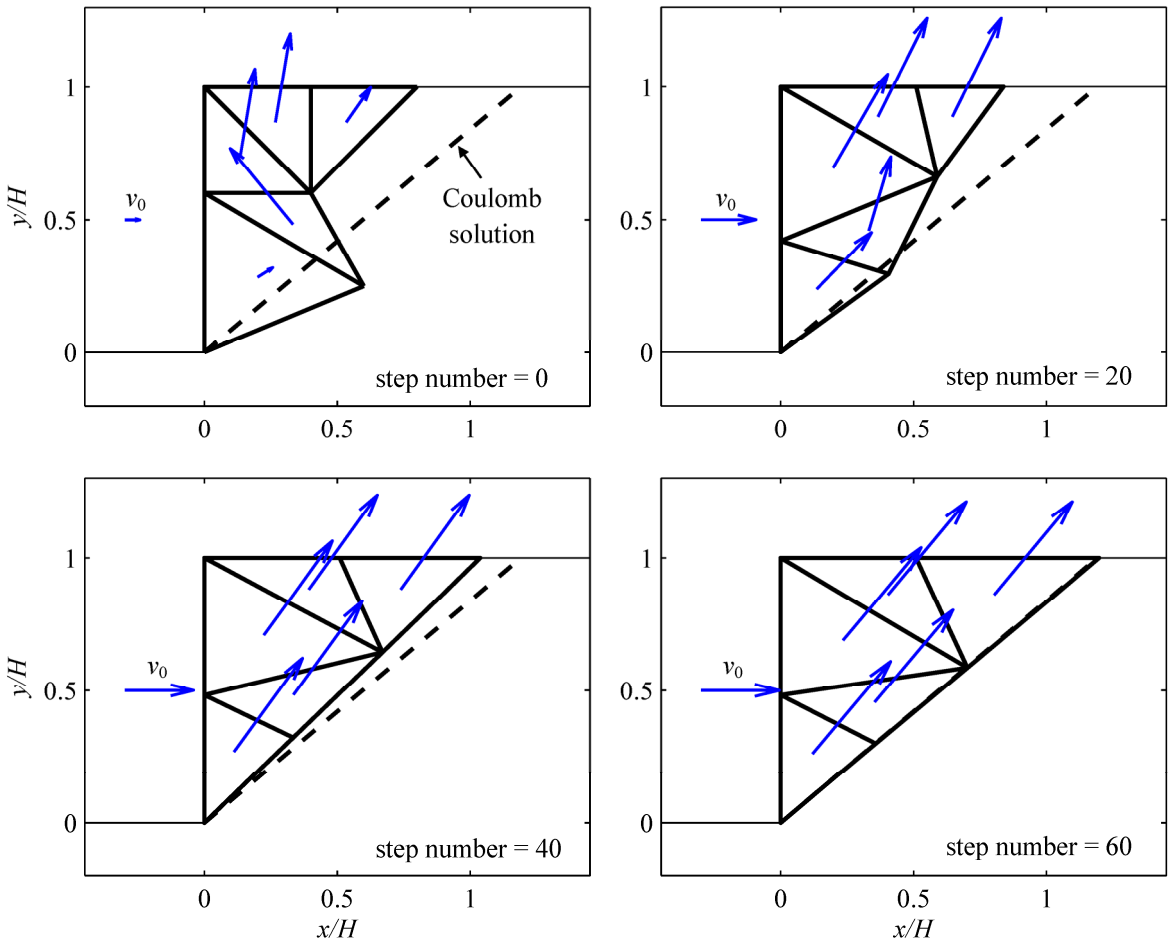

Fig. 2. Finite element mesh and velocities at various perturbation steps for passive earth pressure problem

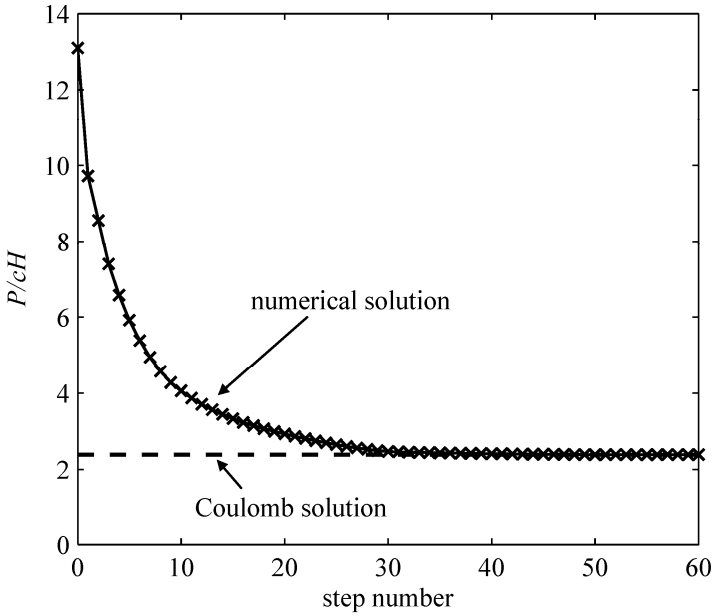

Fig. 3. Limit load as a function of the number of perturbation steps for passive earth pressure problem

The concept behind the proposed method is of potentially great benefit in contemporary numerical limit analysis techniques (cf. Lyamin & Sloan, 2002; Krabbenhøft et al., 2005; Makrodimopoulos & Martin, 2008), and the specific formulation presented provides a valuable alternative to the classical analytical approach to upper bound limit analysis. Namely, the method can be used to compute upper bounds on collapse loads without the need to geometrically construct kinematically admissible mechanisms, which can be a cumbersome process when more than a few rigid blocks are included. Even when a kinematically admissible mechanism can be ascertained analytically, a nonlinear optimization scheme is often needed to determine the optimal values of the free variables involved, and this too is usually a nontrivial endeavor. It should be evident that the formulation proposed in this paper can be applied to mechanisms involving a virtually arbitrary number of elements, and the solution to the corresponding sequence of optimization problems can be found in a matter of seconds using second-order cone programming.

ACKNOWLEDGEMENT

Financial support for this research was provided by the Australian Research Council (grant number FL0992039) in the form of an Australian Laureate Fellowship awarded to Prof. Scott Sloan.

REFERENCES

Anderheggen, E. & Knöpfel, H. (1972), "Finite element limit analysis using linear programming." Int. J. Solids Struct., Vol. 8(12), 1413-1431.

Bottero A., Negre, R., Pastor, J. & Turgeman, S. (1980), "Finite element method and limit analysis theory for soil mechanics problems". Comput. Meth. App. Mech. Eng., Vol. 22(1), 131-149.

Chen, J., Yin, J.-H. & Lee, C.F. (2003), "Upper bound limit analysis of slope stability using rigid finite elements and nonlinear programming". Can. Geotech. J., Vol. 40(4), 742-752.

Chen, W.F. (1975). Limit Analysis and Soil Plasticity, Elsevier, Amsterdam.

Hambleton, J.P. & Drescher, A. (2011), "Approximate model for blunt objects indenting cohesive-frictional material". Int. J. Numer. Anal. Methods Geomech., (in press).

Hambleton, J.P. & Sloan, S.W. (2011), "A coordinate perturbation method for optimization of collapse mechanisms in upper bound limit analysis." Int. J. Solids Struct., (to be submitted).

Krabbenhøft, K., Lyamin, A.V., Hjiaj, M. & Sloan, S.W. (2005), "A new discontinuous upper bound limit analysis formulation". Int. J. Numer. Meth. Eng., Vol. 63(7), 1069-1088.

Lyamin, A.V., Krabbenhøft, K., Hjiaj, M. & Sloan, S.W. (2004), "Discontinuous velocity field for general yield criteria". In: Numerical Models in Geomechanics–NUMOG IX, Pande, G. & Pietruszczak, S. (eds.), Taylor & Francis, London., pp. 291-296.

Lyamin, A.V. & Sloan, S.W. (2002), "Upper bound limit analysis using linear finite elements and non-linear programming". Int. J. Numer. Anal. Methods Geomech., Vol. 26(2), 181-216.

Maciejewski, J. & Jarzębowski, A. (2004), "Application of kinematically admissible solutions to passive earth pressure problems". Int. J. Geomech., Vol. 4(2), 127-136.

Makrodimopoulos, A. & Martin, C.M. (2007), "Upper bound limit analysis using simplex strain elements and second-order cone programming". Int. J. Numer. Anal. Methods Geomech., Vol. 31(6), 835-865.

Makrodimopoulos, A. & Martin, C.M. (2008), “Upper bound limit analysis using discontinuous quadratic displacement fields”. Commun. Numer. Methods Eng., Vol. 24(11), 911-927.
Michalowski, R.L. (1997), “An estimate of the influence of soil weight on bearing capacity using limit analysis”. Soils and Foundations, Vol. 37(4), 57-64.
Michalowski, R.L. (2004), “Limit loads on reinforced foundation soils”. J. Geotech. Geoenviron. Eng., Vol. 130(4), 381-390
Michalowski, R.L. (2007), “Displacements of multiblock geotechnical structures subjected to seismic excitation”. J. Geotech. Geoenviron. Eng., Vol. 133(11), 1432-1439.
Sloan, S.W. & Kleeman, P.W. (1995), “Upper bound limit analysis using discontinuous velocity fields”. Comput. Meth. App. Mech. Eng., Vol. 127(1-4), 293-314.
Smith, C.S. & Gilbert, M. (2007), “Application of discontinuity layout optimization to plane plasticity problems”. Proc. R. Soc. A, Vol. 463(2086), 2461-2484.
Soon, S.-C. & Drescher, A. (2007), “Nonlinear failure criterion and passive thrust on retaining walls”. Int. J. Geomech., Vol. 7(4), 318-322.
Soubra, A.-H. (1999), “Upper-bound solutions for bearing capacity of foundations”. J. Geotech. Geoenviron. Eng., Vol. 125(1), 59-68.
Sturm, J.F. (1999), “Using SeDuMi 1.02, A Matlab toolbox for optimization over symmetric cones”. Optim. Methods Softw., Vol. 11(1), 625-653.